DOI: 10.1002/adma.200700399

The Inner Shell Influence on the Electronic Structure of Double-Walled Carbon Nanotubes**

By *Yann Tison*, *Cristina E. Giusca*, *Vlad Stolojan*, *Yasuhiko Hayashi*, and *S. Ravi P. Silva**

Although carbon nanotubes have been successfully incorporated into nanodevices such as single electron transistors,[1,2] logic gates,[3] biosensors[4] or interconnects,[5] much work still needs to be performed in order to fully comprehend their electronic structure, and thereby their transport properties, down to the nanometer scale, as stated by Bourlon et al. recently in the case of multi-walled carbon nanotubes.[6] In this respect, Scanning Tunneling Microscopy (STM) and Scanning Tunneling Spectroscopy (STS) appear to be ideal techniques to deliver such detail because of their extreme spatial resolution coupled with analytical ability. For instance, STM has been successfully used to determine the structural properties (diameters and chiral indices) of single-walled carbon nanotubes (SWNTs) and to compare their electronic structure from STS spectra with theoretical predictions.[7,8] More recently, the properties of multi-walled carbon nanotubes (MWNTs) have also been investigated using STM and STS[9] showing the presence of an interlayer interaction. To achieve a better understanding of the electronic structure of MWNTs, it is now important to study carbon nanotubes with a known and controlled number of walls. Double-walled carbon nanotubes (DWNTs) are the perfect model system, as they are the smallest multi-walled nanotubes and, therefore, have the simplest electronic structure amongst all MWNTs.

In recent years, several techniques have been used to synthesize double-walled carbon nanotubes. Arc-discharge methods have been used but the samples contain catalyst particle and traces of amorphous carbon.[10,11] CVD methods involving different catalysts, such as iron particles[12–14] or $Mg_{0.9}Co_{0.1}O$ solid solutions[15] are also suitable methods of synthesizing DWNTs. These techniques usually lead to a mixture of SWNTs, DWNTs and wider tubes, displaying a broad range of diameters. A more original synthesis method consists of a structural change of C_{60} peapod structures (i.e., chains of fullerenes inserted into single walled carbon nanotubes) to double-walled carbon nanotubes.[16,17]

The structural properties of double-walled carbon nanotubes have been investigated by high resolution transmission electron microscopy (HRTEM),[18–23] Raman spectroscopy,[16,24,25] and first principle theoretical calculations.[26] These works all show that the interwall spacing varies from 0.34 nm, close to the interlayer distance in graphite (0.335 nm), to 0.42 nm. The electronic structure of DWNTs has also attracted interest. For instance, a few experimental studies involving Raman spectroscopy,[24,25] or HRTEM combined with $I(V)$ measurements,[18] or NMR spectroscopy,[27] have been undertaken in order to link the electronic and transport properties of DWNTs to their structural parameters. The electronic structure of DWNTs bundles has also been investigated by photoelectron spectroscopy,[28] revealing van der Waals interactions between the tubes in a bundle. Many theoretical studies have also been performed recently,[26,29–38] confirming the presence of an interwall interaction and investigating its effect on the electronic structure,[30,35,36] the transport properties[32] and the mechanical properties[37,38] of double-walled nanotubes. In this paper, we report the study of the structural and electronic properties of double-walled carbon nanotubes deposited on a gold substrate using both STM and STS. The influence of the inner shell on the electronic structure and the transport properties of double-walled carbon nanotubes is discussed.

The structural properties of double-walled carbon nanotubes were determined using HRTEM and atomically resolved STM. As shown on Figure 1, the HRTEM images we

[*] Prof. S. R. P. Silva, Dr. Y. Tison,[+] Dr. C. E. Giusca, Dr. V. Stolojan
Nano-Electronics Centre, Advanced Technology Institute
University of Surrey
Guildford, Surrey GU2 7XH (UK)
E-mail: s.silva@surrey.ac.uk
Dr. Y. Hayashi
Nagoya Institute of Technology
Gokiso-cho, Showa-ku, Nagoya, 466-8555 (Japan)
[+] Present address: CAMD, Departmant of Physics, Technical University of Denmark, 2800 Kgs. Lyngby, Denmark.

[**] The authors are grateful to Dr. Paul Smith, Nano-Electronics Centre, for useful discussions and to Dr. Ewa Borowiak-Palen, Szczecin University of Technology, Poland, for her help regarding the purification of carbon nanotubes. This work is funded by the EPSRC through the Carbon Based Electronics program and the Portfolio Partnership Award.

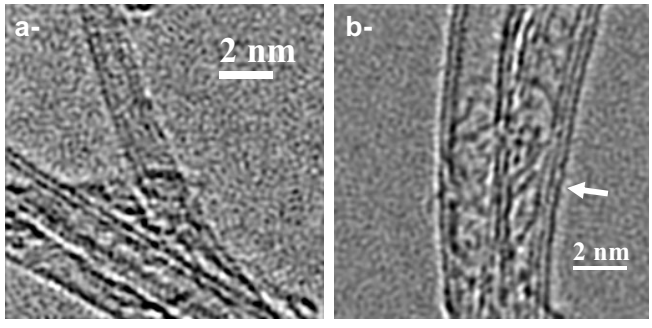

Figure 1. a) HRTEM image of a bundle of double-walled carbon nanotubes; b) HRTEM image of a triple-walled carbon nanotube (indicated by the white arrow) next to a DWNT.

ADVANCED MATERIALS

obtained show clean double-walled carbon nanotubes, with little contamination by amorphous carbon. Outer diameters varying between 1.9 nm and 2.6 nm have been measured. According to our measurements, the interwall spacing varies between 0.30 and 0.54 nm which is in good agreement with results published in the literature.[18–23] The presence of triple-walled carbon nanotubes has also been observed, as indicated on Figure 1b.

Atomically-resolved STM images have been obtained for more than 20 tubes and an example is presented on Figure 2. The diameter of this tube has been determined as the average of ten measurements extracted from different height profiles. Figure 2b displays an example of height profile that shows the diameter of the tube is 2.06 ± 0.05 nm. For the outer wall of this tube, we have also been able to estimate the chiral angle at 21° using the method proposed by Wildöer et al.[7] The chiral indices corresponding to these values are (19,11). Other tubes were analyzed using the same method and we measured diameters varying from 1.5 to 2.9 nm, which are consistent with the HRTEM results presented above and with the data previously reported in the literature,[18–23] with chiral angles varying between 4 and 30°.

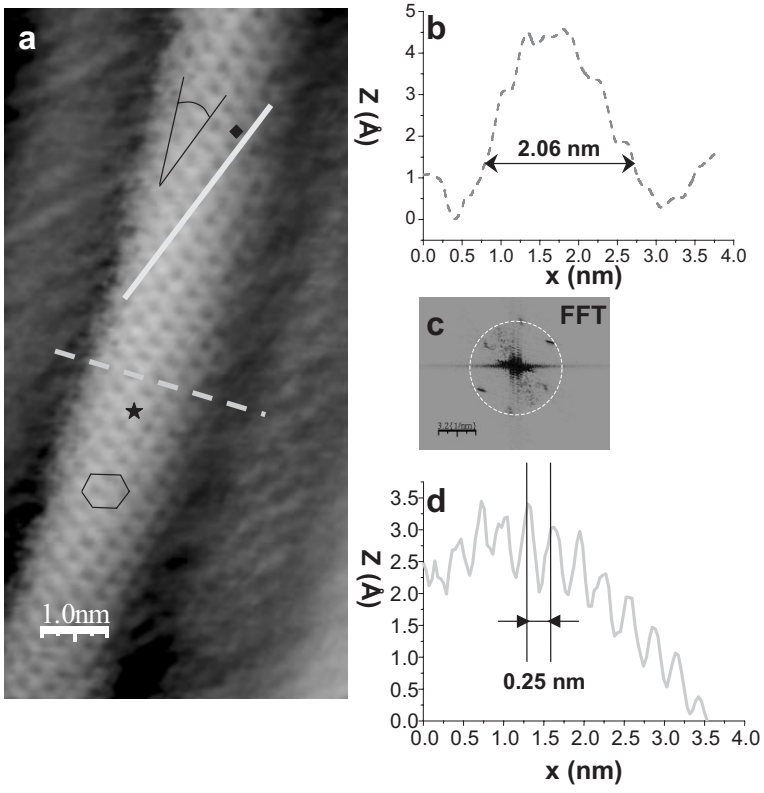

Figure 2. a) Atomically resolved STM image of a DWNT (V_{sample}= 130 mV, I_{tun}= 130 pA), the chiral angle is represented on the image; the black symbols (star and diamond) correspond to the location of the STS measurements presented on Figure 3; b) height profile recorded along the solid line on Figure 3a; c) plot of the Fast Fourier Transform (FFT) for this image highlighting the hexagonal symmetry of the lattice, the dashed circle corresponds to a lattice spacing of 0.25 nm; d) Height profile, plotted along the dashed line on the image (Figure 2a), showing a lattice spacing of 0.25 nm.

One might also note a discrepancy between the diameter (2.06 nm) and the height (between 0.4 and 0.5 nm) measured on the profile extracted from the STM image (Fig. 2b). This effect has recently been discussed by Park et al.[39] and has been attributed to two main factors: the geometrical convolution between the STM tip and the nanotube, and the different tunneling distances between the STM tip and the gold substrate or the double-walled nanotube. In our opinion, the convolution effect is negligible with regard to the differences in terms of tunneling distance for several reasons. Firstly, the use of a blunt STM tip (which would be the main reason for a prominent convolution effect) would lead to a large overestimation of the tubes' diameter.[40] Consequently, the results of the STM measurements would not be consistent with the values obtained during the TEM experiments. Secondly, according to the model proposed by Tersoff and Hamann,[41] the tunneling current is dependent on the local density of states (LDOS) in the vicinity of the Fermi edge. As these LDOS are different for the gold substrate and the DWNTs, the tunneling distances should not be identical in our experimental condition (constant current imaging).[40]

In terms of periodicity, both the image (Fig. 2a) and its Fast Fourier Transform (FFT – Fig. 2c) display a hexagonal lattice. One might notice that the hexagons appear elongated along the tube's circumference. This distortion has previously been reported for multi-walled carbon nanotubes[9] and is associated with small changes of the tip-sample arrangement, due to the tube's morphology. The height profile (Fig. 2d), recorded along the dashed line on the image (Fig. 2a), exhibits a lattice parameter of 0.25 ± 0.01 nm.

The lattice parameter we measured (0.25 nm) is consistent with the results previously reported for larger MWNTs.[9] However, it doesn't correspond to the interatomic distance observed for single-walled carbon nanotubes (0.14 nm).[7,8] This behavior is similar to the one evidenced by the STM images of highly oriented pyrolytic graphite (HOPG)[42] for which only one half of the carbon atoms on the surface are observed. The STM pattern of HOPG results from both the stacking of the graphene sheets and the presence of an interlayer interaction. Two non-equivalent carbon sites are observed on the surface: one is located above a carbon atom of the underlying graphene sheet (site A) and the other is not (site B). Whereas the interlayer interaction does not affect the electronic states which appear in the vicinity of the Fermi edge for the carbon atoms in sites B, it results in a depletion of electronic states around the Fermi level in the case of the carbon atoms located on sites A. Therefore, the STM images of HOPG show the lattice corresponding to the carbon atoms located in sites B,[42] which exhibit the largest density of

states (DOS) at the Fermi level. In the case of DWNTs, although HRTEM results show that there is no systematic correlation between the atomic positions in the neighboring shells,[21] the observation of a 0.25 nm lattice parameter shows that the carbon atoms can be locally arranged according to the AB stacking observed for HOPG. Furthermore, the modification of the surface electronic states confirms the presence of an interwall interaction similar to the one observed in HOPG.

Finally, it is important to note that, despite the acid treatment, we have not observed any trace of functionalized groups, such as –OH or –COOH, on the atomically resolved images of double-walled carbon nanotubes. This is not surprising if we consider that the STM tip is a local probe and that only a small fraction of the tubes' surface has been imaged with atomic resolution. Furthermore, impurities such as amorphous carbon or remaining catalyst particles are more likely to be attached to functionalized fractions of the nanotubes than to the unmodified parts analyzed here. Hence, it would be difficult to obtain clear atomically-resolved images of the functionalized areas of the nanotubes.

In order to investigate the electronic structure of DWNTs, STS measurements have been performed on different locations for more than 10 tubes. The normalized differential conductance ((V/I) $(\mathrm{d}I/\mathrm{d}V)$), corresponding to a spectrum of the local density of states, has been plotted for each tube. As an example, on Figure 3a and b, we show typical curves obtained for the tube presented on Figure 2. The symbols (star and diamond) on the STM image (Fig. 2a) correspond to the location of the $I(V)$ measurement.

Both tunneling spectra exhibit two main bands located between –0.95 V and –0.18 V and between +0.17 V and +0.90 V for the curve on Figure 3a; and between –0.75 V and –0.18 V and between +0.17 V and +0.75 V for Figure 3b. For both curves, the gap separating these contributions has been estimated at 0.35 eV. Several extra features, such as peaks or shoulders, are present with opposite energies in both the filled states (i.e., at negative sample bias voltage) and the empty states (i.e., at positive sample bias voltage), as indicated on the curves. Furthermore, for both spectra, the presence of a non-zero density of states is observed in the vicinity of the Fermi edge, indicative of metallic behavior.

We must highlight that a finite DOS has been observed for all the double-walled nanotubes we have studied using STS. Even if the number of tubes we analyzed is not sufficient to perform statistical calculations, this result confirms previous reports showing that DWNTs can exhibit metallic behavior.[18,27]

Since STM and STS are sensitive to surface states and $(n - m)$ is not a multiple of 3 for the outer shell of the tube presented in Figure 2, the presence of a non-zero DOS at the Fermi level was not expected for the STS spectra on Figure 3. This inconsistency shows that the influence of the inner tube has to be considered in order to explain the results obtained with STS for DWNTs. In this respect, a detailed analysis of the tunneling spectra has been undertaken.

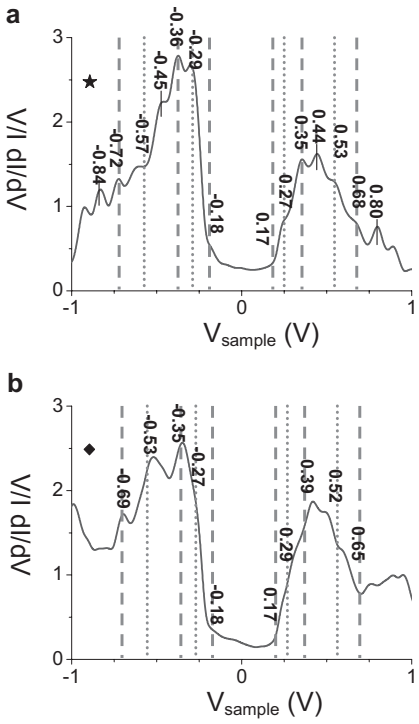

Figure 3. a) Normalized differential conductance (V/I dI/dV) plot recorded at the point represented by a star on the STM image (Fig. 2a); b) Normalized differential conductance (V/I dI/dV) plot recorded at the point represented by a diamond on the STM image (Fig. 2a). The location of the Van Hove singularities for a semi-conducting shell with a diameter of 2.06 nm (resp. 1.36 nm) is represented by the dashed (resp. dotted) lines.

The energy of the Van Hove singularities for a (19,11) semiconducting tube has been estimated using the relation proposed by Charlier and Lambin.[43] In this model, the Van Hove singularities arise at:

$$E_1 = \pm (a_{c\text{-}c})\gamma_0/d,\ E_2 = \pm 2(a_{c\text{-}c})\gamma_0/d,\ E_3 = \pm 4(a_{c\text{-}c})\gamma_0/d...$$

where + or – determines whether the singularity belongs to the conduction or valence band, $a_{c\text{-}c}$ is the interatomic spacing in a nanotube (0.142 nm), γ_0 is the C–C tight-binding overlap energy (chosen at 2.7 eV as proposed by Wildöer et al.[7]) and d is the diameter of tube.

According to this model, the Van Hove singularities should be observed at ± 0.19 eV, ± 0.37 eV and ± 0.73 eV for a single-walled carbon nanotube with a diameter of 2.06 nm. As highlighted by dashed lines on Figure 3, these values correspond to some of the peaks and shoulders observed on the spectra obtained experimentally.

A possible explanation for the presence of the other features may be the fact that they arise from the inner tube. The diameter of the inner shell can be estimated by subtracting the double of the interwall distance (0.35 nm) to the diameter of the outer shell (2.06 nm). In our case, we expect the diame-

ADVANCED MATERIALS

ter of the core tube to be close to 1.36 nm. If this inner tube were metallic, the equation $E_1 = \pm 3(a_{c\text{-}c})\gamma_0/d$[43] would be valid for determining the energy associated with the first Van Hove singularities. For a 1.36 nm diameter metallic shell, the first Van Hove singularity would be observed at ± 0.85 eV; peaks corresponding to these values are observed on the curve presented on Figure 3a but not on the curve shown on Figure 3b. In the case of a semi-conducting inner shell, the energy associated with the Van Hove singularities would be estimated by the equations: $E_1 = \pm (a_{c\text{-}c})\gamma_0/d$, $E_2 = \pm 2(a_{c\text{-}c})\gamma_0/d$, $E_3 = \pm 4(a_{c\text{-}c})\gamma_0/d$... as previously described.[43]

For a 1.36 nm semi-conducting tube, the first two Van Hove singularities should be observed at ± 0.28 eV and ± 0.56 eV, features which are indeed observed on both curves and highlighted by dotted lines on Figure 3. Hence, we believe the inner wall of this double-walled tube corresponds to a semi-conducting single-walled nanotube with a diameter close to 1.36 nm.

This analysis, however, doesn't explain the presence of extra features, such as the peaks observed at ± 0.45 V on Figure 3a. They could correspond to a localized defect on the inner tube or the back side of the outer shell or to the occurrence of additional Van Hove singularities due to a loss of degeneracy in double-walled tubes compared to single-walled, as highlighted in a recent study involving Raman spectroscopy.[25] In that case, these contributions may still be present on Figure 3b, but they would not be resolved from the peaks corresponding to the Van Hove singularities arising around ± 0.37 eV for the outer tube.

To summarize, the measurements we performed show that the Van Hove singularities of both the inner and the outer shells can be observed for double-walled carbon nanotubes during STS measurements. In the particular case we present here, both shells appear to be semi-conducting whereas the STS spectra display a non-zero DOS at the Fermi level, typical of a metallic nanotube. This result is consistent with the results reported by Kociak et al.[18] who determined the chiral indices of both shells of a DWNT using TEM, showed this tube constituted of two semi-conducting SWNT and recorded $I(V)$ curves typical of metallic behavior.

The origin of the behavior we observe during the STS study of DWNTs, i.e., the finite DOS at the Fermi edge and the presence of the Van Hove singularities of both shells on the tunneling spectra, is still unclear. In our opinion, both effects arise from an interaction between the π systems of the walls, as previously observed for MWNTs[9] and modeled in the case of DWNTs.[30,35,36] The hypothesis of an intershell interaction is also supported by the periodicity of 0.25 nm on the STM images of the DWNTs, similar to that observed on STM images of graphite, and due to an interlayer interaction, as discussed earlier. Due to this interaction, the electronic structure of the DWNTs cannot be described as independent wave functions corresponding to the inner and outer shells, but by a convolution or combination of states arising from both shells, with an interaction term also included. The electronic structure and the transport properties of DWNTs have been debated for more that a decade. Early theoretical work from Saito et al.[29] demonstrated that double-walled carbon nanotube containing at least one metallic shell exhibit a metallic behavior, a prediction which we could confirm during the STM/STS study of a different DWNT.[44] Furthermore, several experimental studies, using techniques such as $I(V)$ measurements coupled with HRTEM,[18] Raman spectroscopy[45] or Nuclear Magnetic Resonance[27] and the STM/STS results reported here, show the presence of a finite density of states at the Fermi edge for DWNTs constituted of two semi-conducting single-walled carbon nanotubes. More recent theoretical studies have shown that this interaction induces a redistribution of electronic states to the inter-tube region,[30] states similar to the interlayer states observed for graphite around the Fermi edge,[46] and that it can induce metallicity for DWNTs constituted of semi-conducting SWNTs.[35,36] Even if those theoretical studies are limited to zigzag or armchair shells and need confirmation for chiral systems, we can assume that the STS results are characteristic of the electronic states resulting from the interwall interaction and therefore exhibit contributions from both shells and from the density of states appearing at the Fermi edge.

Another interesting point is the lattice registry between the two shells and its relation with the interwall interaction. For instance, Charlier and Michenaud have used Density Functional Theory in order to determine the optimal intershell distance at approximately 0.34 nm and also showed that some stacking sequences are energetically favored.[26] More recently, Kolmogorov and Crespi proposed a potential based on a Lennard–Jones approach in order to account for the registry-dependence of the intershell interaction.[47,48] This K–C potential was introduced in a DFT calculation and the authors demonstrated that the double-walled carbon nanotube's geometry, in particular the lattice registry between the shells, influences the energy barriers for sliding or rotating a tube with respect to the other.[48] In a slightly different approach, Bellarosa et al. mapped the potential energy distribution of carbon nanotubes embedded in or embedding three widely studied carbon nanotubes and showed that some combinations of chiral indices are energetically favored.[49] In a similar manner, the K–C potential has been used to determine the interlayer potential of double-walled carbon nanotubes and it is found that for a given set of chiral indices (n,m) of the inner tube, the optimum outer tube is described by the chiral indices $(n+9, m)$ or $(n+10, m)$.[50] As a consequence, the most probable chiral indices for the inner shell of the double-walled carbon nanotube studied in this paper would be (11,9) and (11,10) whose properties, extracted from the work of Akai and Saito,[51] are reported in Table 1.

In the case of the (11,9)@(19,11) DWNT, the interwall distance would be 0.35 nm whereas it would be 0.32 nm for the (11,10)@(19,11) system, both in the range determined from the HRTEM measurements (0.30–0.54 nm). Furthermore, for both the (11,9) and (11,10) tubes, the Van Hove Singularities are predicted to arise at energies of ± 0.27 eV and ± 0.52 eV, which are within experimental error from the experimental values.[44] It is therefore not possible to determine which of

Table 1. Chiral angles, diameters and energetic positions of the first Van Hove singularities of the (11,9) and (11,10) single-walled carbon nanotubes, most probable candidates for being the inner tube of the double-walled carbon nanotube presented here.

Inner Tube	Chiral Angle	Diameter	1st VHS	2nd VHS
(11,9)	26.7°	1.356 nm	±0.27 eV	±0.52 eV
(11,10)	28.4°	1.422 nm	±0.27 eV	±0.52 eV

these two candidate solutions is the most likely to correspond to the inner wall. However, as previous HRTEM experiments demonstrated, there is no systematic correlation between the chiral angle of both shells.[21] Moreover, the energy difference between the energetically favored couple of chiral indices and the other cases is smaller than 5 meV/atom.[50] For these reasons, one cannot exclude the other possible candidates from being the inner tube in this double-walled nanotube, such as the tubes described by the indices (15,4), (14,6), or (12,7) for example. To fully confirm the correlation between the STS spectra and the chiral indices of both the inner and the outer tube, one would have to perform HRTEM, atomically resolved STM imaging and STS on the same double-walled carbon nanotube.

We now discuss the consequences of the interwall interaction on the conduction in multiwalled carbon nanotubes. The pathway of electrons through a multi-walled carbon nanotube with a contact on the outer wall is still uncertain. Early results suggested that the current is confined to the outermost layers.[52] However, more recently, an intershell conductance attributed to tunneling through orbitals of nearby shells has been reported.[53] Furthermore, Collins et al.[54,55] have estimated the contribution of the different shells by progressively thinning multi-walled carbon nanotubes. Their original technique allowed them to demonstrate a flow of current through the inner shells. Due to the electronic interaction, the electronic structure of multi-walled carbon nanotubes is not simply the sum of a number of isolated single-walled tubes. One has to consider the tube as complex system of interacting shells to fully investigate their transport properties. In particular, the charge transfer to the interwall spacing evidenced by Miyamoto et al.[30] probably facilitates the tunneling of electrons between neighboring shells. Furthermore, due to the interwall interaction and the charge transfer, the transport properties of a shell in a MWNTs will be different from the properties of an isolated SWNT with the same diameter and chirality. We are currently performing a theoretical study based on DFT calculations, in order to investigate the nature of this interaction, as well as its consequences, and possibly help determine whether the conduction in MWNTs is driven by a Luttinger liquid behavior[56] or by Coulomb blockade.[57]

In summary, we studied the structural properties and the electronic structure of double-walled carbon nanotubes using HRTEM, STM and STS measurements. The HRTEM measurements allowed us to check the number of walls in the DWNTs and to estimate their diameter and interwall spacing. Atomic resolution imaging was achieved for a number of tubes and allowed us to determine the diameter, the chiral angle and the periodicity of the outer shell; these results also allowed us to determine the chiral indices of this outer wall. During STS experiments, the Van Hove singularities of both the outer and the inner shell could be observed on the normalized differential conductance curves. The STS results also showed that the double-walled carbon nanotube presented here consist of two semi-conducting single-walled carbon nanotubes and exhibits a finite density of states near the Fermi level in the overall measurement. The behavior, we believe, is related to the presence of an interwall interaction which results in an accumulation of electronic states in the inter-tube region, at energies close to the Fermi level. This interaction also induces a modification of the periodicity of the STM image (0.25 nm) with regard to the results obtained for single-walled carbon nanotubes. Moreover, lattice registry effects are discussed and attempts of identifying the chiral indices of the inner shell have been made on the basis of previous theoretical studies. The characterization of this interwall interaction and its consequences, in particular for the case of chiral shells is an area that needs much further study and this work presents direct experimental evidence as to the importance of their effect which has a profound influence on the optoelectronic properties of nanowires.

Experimental

The double-walled carbon nanotubes used in this work have been purchased from Carbon Nanotechnologies Incorporated. Prior to the experiment, the nanotubes have been acid treated (reflux in HNO_3, 1 mol.L^{-1} for 24 hours) and oxidized in air at 250 °C in order to remove most of the catalyst and amorphous carbon particles. The purified DWNTs were then dispersed in 1,2-dichloroethane (1 mg mL^{-1}) and sonicated for 2 hours before TEM and STM experiments were performed. To prepare the STM sample, 2–3 drops of the sonicated dispersion were deposited on a gold (111) surface. The sample was then mounted on a sample plate and introduced into the Ultra High Vacuum Scanning Tunneling Microscope (UHV-STM).

The STM and STS experiments were performed at room temperature in a commercial UHV-STM (Omicron VT Multiscan STM) equipped with a SEM column. Electrochemically-etched tungsten tips have been used for this study. During the experiments, the base pressure in the UHV chamber was 2×10^{-11} mbar. STM images were recorded in constant current mode with the sample biased in the range –0.3 V to 0.3 V and the tunneling current kept at 100 pA. The STM images were processed and analyzed using the WSxM package (WSxM free software available for download at http://www.nanotec.es). The STS measurements were carried out as follows, the position of the STM tip was locked on selected locations of the STM image and $I(V)$ curves were recorded for sample bias varying between –1.00 V and +1.00 V. After the experiment, normalized differential conductance (V/I dI/dV) curves were extracted using the WSxM package.

The HRTEM experiments were carried out on a Philips CM200 TEM (200kV accelerating voltage, LaB_6 source) fitted with a Gatan Imaging Filter (GIF2000). The microscope was calibrated immediately prior to the irradiation experiment and changes in the microscope lenses were kept to a minimum when switching to the nanotubes. Calibration was again verified against the graphite (002), resulting in a measurement error of ± 0.05 Å.

Received: February 14, 2007
Revised: July 6, 2007
Published online: December 11, 2007

[1] H. W. C. Postma, T. Teepen, Z. Yao, M. Grifoni, C. Dekker, *Science* **2001**, *293*, 76.
[2] S. Li, Z. Yu, S.-F. Yen, W. C. Tang, P. J. Burke, *Nano Lett.* **2004**, *4*, 753.
[3] P. R. Bandaru, C. Daraio, S. Jin, A. M. Rao, *Nat. Mater.* **2005**, *4*, 663.
[4] J. Wang, *Electroanalysis* **2004**, *17*, 7.
[5] J. Li, Q. Ye, A. Cassell, H. T. Ng, R. Stevens, J. Han, M. Meyyappan, *Appl. Phys. Lett.* **2003**, *82*, 2491.
[6] B. Bourlon, C. Miko, L. Forró, D. C. Glattli, A. Bachtold, *Semicond. Sci. Technol.* **2006**, *21*, S33.
[7] J. W. G. Wildöer, L. C. Venema, A. G. Rinzler, R. E. Smalley, C. Dekker, *Nature* **1998**, *391*, 59.
[8] T. W. Odom, J.-L. Huang, P. Kim, C. M. Lieber, *Nature* **1998**, *391*, 62.
[9] A. Hassanien, A. Mrzel, M. Tokumoto, D. Tománek, *Appl. Phys. Lett.* **2001**, *79*, 4210.
[10] J. L. Hutchison, N. A. Kiselev, E. P. Krinichnaya, A. V. Krestinin, R. O. Loufty, A. P. Morawsky, V. E. Muradyan, E. D. Obratzova, J. Sloan, S. V. Terekhov, D. N. Zakharov, *Carbon* **2001**, *39*, 761.
[11] T. Sugai, H. Yoshida, T. Shimada, T. Okazaki, H. Shinohara, *Nano Lett.* **2003**, *3*, 769.
[12] L. Ci, Z. Rao, Z. Zhou, D. Tang, X. Yan, Y. Liang, D. Liu, H. Yuan, W. Zhou, G. Wang, W. Liu, S. Xie, *Chem. Phys. Lett.* **2002**, *359*, 63.
[13] W. Ren, F. Li, J. Chen, S. Bai, H.-M. Cheung, *Chem. Phys. Lett.* **2002**, *359*, 196.
[14] J. Cummings, W. Mickelson, A. Zettl, *Solid State Commun.* **2003**, *126*, 359.
[15] E. Flahaut, R. Bacsa, A. Peigney, C. Laurent, *Chem. Commun.* **2003**, 1442.
[16] S. Bandow, M. Takizawa, K. Hirahara, M. Yudasaka, S. Iijima, *Chem. Phys. Lett.* **2001**, *337*, 48.
[17] M. Abe, H. Kataura, H. Kira, T. Kodama, S. Suzuki, Y. Achiba, K.-I. Kato, M. Takada, A. Fujiwara, K. Matsuda, Y. Maniwa, *Phys. Rev. B* **2003**, *68*, 041405(R).
[18] M. Kociak, K. Suenaga, K. Hirahara, Y. Saito, T. Nakahira, S. Iijima, *Phys. Rev. Lett.* **2002**, *89*, 155501.
[19] M. Kociak, K. Hirahara, K. Suenaga, S. Iijima, *Eur. Phys. J. B* **2003**, *32*, 457.
[20] H. Zhu, K. Suenaga, A. Hashimoto, K. Urita, S. Iijima, *Chem. Phys. Lett.* **2005**, *412*, 116.
[21] A. Hashimoto, K. Suenaga, K. Urita, T. Shimada, T. Sugai, S. Bandow, H. Shinohara, S. Iijima, *Phys. Rev. Lett.* **2005**, *94*, 045504.
[22] J. M. Zuo, I. Vartanyants, M. Gao, R. Zhang, L. A. Nagahara, *Science* **2003**, *300*, 1419.
[23] P. M. F. J. Costa, S. Friedrichs, J. Sloan, M. L. H. Green, *Carbon* **2004**, *42*, 2527.
[24] J. Wei, B. Jiang, X. Zhang, H. Zhu, D. Wu, *Chem. Phys. Lett.* **2003**, *376*, 753.
[25] W. Ren, F. Li, P. Tan, H.-M. Cheng, *Phys. Rev. B* **2006**, *73*, 115430.
[26] J.-C. Charlier, J.-P. Michenaud, *Phys. Rev. Lett.* **1993**, *70*, 1858.
[27] P. M. Singer, P. Wzietek, H. Alloul, F. Simon, H. Kuzmany, *Phys. Rev. Lett.* **2005**, *95*, 236403.
[28] H. C. Choi, S. Y. Kim, W. S. Jang, S. Y. Bae, J. Park, K. L. Kim, K. Kim, *Chem. Phys. Lett.* **2004**, *399*, 255.
[29] R. Saito, G. Dresselhaus, M. S. Dresselhaus, *J. Appl. Phys.* **1993**, *73*, 494.
[30] Y. Miyamoto, S. Saito, D. Tománek, *Phys. Rev. B* **2001**, *65*, 041402(R).
[31] R. Saito, R. Matsuo, T. Kimura, G. Dresselhaus, M. S. Dresselhaus, *Chem. Phys. Lett.* **2001**, *348*, 187.
[32] A. Hansson, S. Stafström, *Phys. Rev. B* **2003**, *67*, 075406.
[33] Y. H. Ho, C. P. Chang, F. L. Shyu, R. B Chen, S. C. Chen, M. F. Lin, *Carbon* **2004**, *42*, 3159.
[34] J. Chen, L. Yang, *J. Phys. Condens. Matter* **2005**, *17*, 957.
[35] V. Zólyomi, A. Rusznyák, J. Kürti, A. Gali, F. Simon, H. Kuzmany, A. Szabados, P. R. Surjan, *arXiv:cond-mat/0603407* **2006**.
[36] V. Zólyomi, Á. Rusznyák, J. Kürti, Á. Gali, F. Simon, H. Kuzmany, Á. Szabados, P. R. Surján *Phys. Status Solidi B* **2006**, *243*, 3476.
[37] C. Li, T.-S. Chou, *Mech. Mater.* **2004**, *36*, 1047.
[38] E. Bichoutskaia, M. I. Heggie, A. M. Popov, Y. E. Lozovik, *Phys. Rev. B* **2006**, *73*, 045435.
[39] M. H. Park, J. W. Jang, C. E. Lee, C. J. Lee, *Appl. Phys. Lett.* **2005**, *86*, 023110.
[40] L. P. Biró, S. Lazarescu, P. Lamblin, P. A. Thiry, A. Fonseca, J. B. Nagy, A. A. Lucas, *Phys. Rev. B* **1997**, *56*, 12490.
[41] J. Tersoff, D. R. Hamann, *Phys. Rev. Lett.* **1983**, *50*, 1998.
[42] S. Magonov, M.-H. Whangbo, *Surface Analysis with STM and AFM*, VCH, Weinheim **1996**, Ch. 5.
[43] J.-C. Charlier, P. Lambin, *Phys. Rev. B* **1998**, *57*, 15037.
[44] C. E. Giusca, Y. Tison, V. Stolojan, E. Borowiak-Palen, S. R. P Silva, *Nano Lett.* **2007**, *7*, 1232.
[45] R. Pfeiffer, F. Simon, H. Kuzmany, V. N. Popov, V. Zólyomi, J. Kürti, *Phys. Status Solidi B* **2006**, *243*, 3268.
[46] M. Posternak, A. Baldereschi, A. J. Freeman, E. Wimmer, M. Weinert, *Phys. Rev. Lett.* **1983**, *50*, 761.
[47] A. N. Kolmogorov, V. H. Crespi, *Phys. Rev. Lett.* **2000**, *85*, 4727.
[48] A. N. Kolmogorov, V. H. Crespi, *Phys. Rev. B* **2005**, *71*, 235415.
[49] L. Bellarosa, E. Bakalis, M. Melle-Franco, F. Zerbetto, *Nano Lett.* **2006**, *6*, 1950.
[50] W. Guo, Y. Guo, *J. Am. Chem. Soc.* **2007**, *129*, 2730.
[51] Y. Akai, S. Saito, *Phys. E* **2005**, *29*, 555.
[52] S. Frank, P. Poncharal, Z.L. Wang, W. A. de Heer, *Science* **1998**, *280*, 1744.
[53] B. Bourlon, C. Miko, L. Forró, D. C. Glattli, A. Bachtold, *Phys. Rev. Lett.* **2004**, *93*, 176806.
[54] P. G. Collins, M. Hersam, M. Arnold, R. Martel, P. Avouris, *Phys. Rev. Lett.* **2001**, *86*, 3128.
[55] P. G. Collins, P. Avouris, *Appl. Phys. A* **2002**, *74*, 329.
[56] R. Egger, *Phys. Rev. Lett.* **1999**, *83*, 5547.
[57] A. Bachtold, M. De Jonge, K. Grove-Rasmussen, P. L. McEuen, M. Buitelaar, C. Schönenberger, *Phys. Rev. Lett.* **2001**, *87*, 166801.